Title

Investigating MRI-Associated Biological Aspects of Racial Disparities in Prostate Cancer for African American and White Men

Authors

Zabihollahy, Fatemeh
Miao, Qi
Naim, Sohaib
et al.

Publication Date

2024-05-15

DOI

10.1002/jmri.29397

Peer reviewed

Investigating MRI-associated Biological Aspects of Racial Disparities in Prostate Cancer for African American and White Men

Fatemeh Zabihollahy[1], PhD, Qi Miao[1,2], MD, Sohaib Naim[1], MS, Ida Sonni[1], MD, Sitaram Vangala[3], MS, Harrison Kim[4], PhD, William Hsu[1], PhD, Anthony Sisk[5], DO, Robert Reiter[6], MD, Steven S. Raman[1], MD, Kyunghyun Sung[1], PhD

[1] Department of Radiological Sciences, David Geffen School of Medicine, University of California, Los Angeles, CA, USA
[2] Department of Radiology, The First Affiliated Hospital of China Medical University, Shenyang City, Liaoning Province, China
[3] Department of Medicine Statistics Core, David Geffen School of Medicine, University of California, Los Angeles, CA, USA
[4] Department of Radiology, University of Alabama at Birmingham, Birmingham, AL, USA
[5] Department of Pathology, David Geffen School of Medicine, University of California, Los Angeles, CA, USA
[6] Department of Urology, David Geffen School of Medicine, University of California, Los Angeles, CA, USA

***Correspondence to:**

Fatemeh Zabihollahy, PhD

Phone: (613) 890-6438

Zabihollahy.f@gmail.com

Grant Support: National Institutes of Health R01-CA248506 and R01-CA272702.

Running Title*:* Investigating MRI-associated Racial Disparity in Prostate Cancer.

Accepted for publication in the Journal of Magnetic Resonance Imaging

ABSTRACT

Background: Understanding the characteristics of multiparametric MRI (mpMRI) in patients from different racial/ethnic backgrounds is important for reducing the observed gaps in clinical outcomes.

Purpose: To investigate the diagnostic performance of mpMRI and quantitative MRI parameters of prostate cancer (PCa) in African American (AA) and matched White (W) men.

Study type: Retrospective.

Subjects: 129 patients (43 AA, 86 W) with histologically proven PCa who underwent mpMRI before radical prostatectomy.

Field strength/sequence: 3.0 T, T2-weighted turbo spin echo imaging, a single-shot spin-echo EPI sequence diffusion-weighted imaging, and a gradient echo sequence dynamic contrast-enhanced MRI with an ultrafast 3D spoiled gradient-echo sequence.

Assessment: The diagnostic performance of mpMRI in AA and W men was assessed using detection rates (DRs) and positive predictive values (PPVs) in zones defined by the PI-RADS v2.1 prostate sector map. Quantitative MRI parameters, including K^{trans} and v_e of clinically significant (cs)PCa (Gleason score ≥ 7) tumors were compared between AA and W sub-cohorts after matching age, prostate-specific antigen (PSA), and prostate volume.

Statistical tests: Weighted Pearson's chi-square and Mann-Whitney U tests with a statistically significant level of 0.05 were used to examine differences in DR and PPV and to compare parameters between AA and matched W men, respectively.

Results: A total number of 264 PCa lesions were identified in the study cohort. The PPVs in the peripheral zone (PZ) and posterior prostate of mpMRI for csPCa lesions were significantly higher in AA men than in matched W men (87.8% vs. 68.1% in PZ, and 89.3% vs. 69.6% in posterior

prostate). The K^{trans} of index csPCa lesions in AA men was significantly higher than in W men (0.25±0.12 vs. 0.20±0.08 min^{-1}; P<0.01).

Data Conclusion: This study demonstrated race-related differences in the diagnostic performances and quantitative MRI measures of csPCa that were not reflected in age, PSA, and prostate volume.

Keywords: Multi-parametric MRI, Prostate cancer, Health disparity

INTRODUCTION

The risk of prostate cancer (PCa) is influenced by race and ethnicity (1). In particular, African American (AA) men in the general US population have a higher likelihood of PCa-related death than White (W) men due to increased incidence and poorer survival after diagnosis (2,3). Multiple studies have suggested that socioeconomic factors and healthcare access may account for the differences(2-6). However, a growing body of literature also shows that genetic and biological factors may also be implicated in developing these discrepancies (7,8). The underlying causes are complex and likely multifactorial (9) and understanding the impact of biological heterogeneity in patients from different racial/ethnic backgrounds is important for reducing the observed gaps in clinical outcomes. However, there is a paucity of studies investigating imaging characteristics or phenotypes associated with aggressive PCa among men from different racial backgrounds.

Multiparametric MRI (mpMRI) allows for the exploration of the biological and molecular characteristics of PCa with a combination of anatomic and functional information. Dynamic contrast-enhanced MRI (DCE-MRI), as part of mpMRI, measures microvascular perfusion by monitoring the dynamic change of MRI contrast agent in the target tissue (10,11). Increased perfusion is associated with a higher grade of PCa, requiring more aggressive management (12). Differences in quantitative DCE-MRI (qDCE) parameters may potentially explain the biological differences noted between AA and W men and ultimately improve the characterization of clinically significant PCa (csPCa) in patients with different ethnic backgrounds (13,14). Also, several studies have shown that AA men present with higher prostate volume (PV) and prostate-specific antigen (PSA) than W men (9,15). Therefore, these clinical variables need to be taken into account to minimize the bias when investigating potential imaging differences between AA and W men.

Thus, the aim of this study was to evaluate the diagnostic performances of mpMRI and to assess differences in quantitative MRI parameters of prostate cancer lesions, investigating imaging characteristics or phenotypes associated with clinically significant PCa between AA and matched W men.

MATERIALS AND METHODS

Study Population

This single institution retrospective study was approved by the local institutional review board (IRB) with a waiver of the requirement for informed consent. It was conducted in compliance with the United States Health Insurance Portability and Accountability Act (HIPAA) of 1996. The initial study cohort comprised 942 consecutive patients who underwent preoperative mpMRI prior to radical prostatectomy from July 2010 to January 2023. We excluded all patients meeting one or more of the following criteria: 1) unknown/missing race information; 2) prior treatment for PCa (e.g., radiation therapy, focal ablation, androgen deprivation therapy); 3) missing mpMRI in 3T scanners; 4) missing preoperative serum prostate-specific antigen (PSA) measurement. After reviewing the electronic medical records, patient age, self-identified race/ethnicity, clinical (serum PSA levels prior to surgery), imaging (mpMRI), and pathology reports were recorded.

We applied a propensity score caliper matching algorithm to match AA to W men in a 1:2 ratio with the variables patient age, PSA, and PV. These clinical variables are known to be associated with the risk factors for PCa diagnosis (16). The differences in age, PSA, PSA density (PSAD), and PV between AA and W populations after propensity score matching are shown in Table 1. The sample size of the AA and W groups was unbalanced, and there was a significant difference in PV,

which can be a confounding factor. Propensity score matching was used to minimize the bias due to the confounding variables when comparing AA and W men, similar to previous studies (17-20). We adjusted age, PSA, and PV covariates, to balance them within the strata of the propensity score between the two groups. A total of 129 AA and W men from the initial cohort of 942 patients were included in the final analysis (Figure 1).

MRI Acquisition and Analysis

The mpMRI was performed on a 3T scanner (Magnetom, Prisma, Skyra, Vida, or Verio; Siemens Healthineers, Erlangen, Germany) with a pelvic external phased array coil, and with or without an endorectal coil (MEDRAD, Indianola, PA., USA), using nearly identical imaging protocols following the European Society of Urogenital Radiology (ESUR) PI-RADS guidelines (21). The mpMRI protocol included T2-weighted turbo spin echo imaging (T2WI), diffusion weighted imaging (DWI), and DCE imaging, as described below. PCa tumors were initially identified on all preoperative mpMRIs by an abdominal imaging fellow and then reviewed by a board-certified attending abdominal radiologist (S.S.R. with 26 years of experience) as part of the standard of care in our institute.

Apparent diffusion coefficient (ADC) maps were generated from DWI acquired with four b values (0/100/400/800 s/mm^2) via the in-line postprocessing (Siemens Healthineers, Erlangen, Germany) using the least-squares curve fitting method. ADC ($\mu mm^2/s$) values were generated by using the mono-exponential decay model, defined by $s = s_0 \cdot e^{-b \cdot ADC}$, where s and s_0 are the pixel values with and without diffusion sensitive gradients, b. High b-value (1,400 s/mm^2) DWI images were also used for mpMRI interpretations based on the PI-RADS v2.1 criteria as part of the standard of care (22).

The DCE-MRI was acquired with an ultrafast 3D spoiled gradient-echo sequence without fat saturation. Five images were acquired before injecting gadopentetate dimeglumine (Magnevist; Bayer, Wayne, NJ) at a dose of 0.1 mmol/kg through a peripheral vein at a rate of 2 mL/sec via a mechanical injector, and approximately 70 images were acquired after that, without delay between the acquisitions, with a temporal resolution of 5-6 seconds. The number of image slices was 20, and the slice thickness was 3.6 mm. The sequence parameters are shown in Table 2.

For quantitative analysis of DCE-MRI, we used the standard Tofts model defined as (23):

$$C_t(t) = K^{trans} \int_0^t C_p(\tau) e^{-k_{ep}(t-\tau)} d\tau,$$

where $C_t(t)$ is the total tissue contrast agent concentration, $C_p(t)$ is the time-varying blood plasma concentration after a bolus of gadolinium is administered, K^{trans} is the volume transfer constant (wash-in rate; min^{-1}), and k_{ep} is the blood influx rate (wash-out rate; min^{-1}). Among multiple arterial input function (AIF) options, a population-averaged Parker AIF was used to obtain K^{trans} and k_{ep} using DCE-MRI images (24,25). The quantitative DCE (qDCE) analysis was performed, blinded to race/ethnicity, using a lab-made software package with MATLAB (MathWorks, Natick, MA), compliant with the Quantitative Imaging Biomarkers Alliance (QIBA) DCE-MRI quantitation profile (26).

Radiology-pathology Correlation

Genitourinary pathology technicians prepared thin-section whole-mount histopathology (WMHP) slices; each prostate gland was in the axial plane, perpendicular to the urethra from anterior to posterior from the apex to the base in 5-mm increments using a 3D printed mold derived from the preoperative MRI. Each whole mount slice was fixed for 24 hours and embedded in paraffin. After

hematoxylin and eosin (H&E) staining, each whole-mount slice was digitally photographed. A genitourinary pathologist (A.S. with 9 years of experience) manually delineated the PCa tumor boundary on each image slice and assigned a Gleason score (GS) and an International Society of Urological Pathology (ISUP) grade for each PCa lesion (27), where GS ≤ 6, 3 + 4 = 7, 4 + 3 = 7, 8 and 9-10, respectively, were reported as five groups, i.e. ISUP grades 1-5. The lesions with ISUP grade ≥ 2 (GS ≥ 3+4) were defined as csPCa.

Each lesion was assigned a PI-RAD score from 1 to 5 indicating the likelihood of clinically significant cancer, from very low, low, intermediate, high and very high. For MRI-positive (PI-RADS ≥ 3) and/or pathology-positive lesions, both an MRI scientist (K.S. with 15 years of experience in analyzing MRI data) and an abdominal radiologist (Q.M. with 5 years of experience in prostate mpMRI interpretation) retrospectively reviewed all cases and manually annotated regions-of-interest (ROIs) encompassing the entire lesion on slices of both the ADC and K^{trans} maps. ADC, K^{trans}, and k_v values were averaged within the volumetric ROIs encompassing the entire lesion on multiple slices. The use of a volumetric average reduces dependencies on potential variations of the lesion annotations (28).

This study focused on the PCa tumors with PI-RADS ≥ 3 and (a) ISUP grades ≥ 2, and (b) index ISUP grades ≥ 2. An MRI-positive and pathology-positive lesion was labeled as true positive (TP). An MRI-positive but pathology-negative lesion was labeled as false positive (FP), while an MRI-negative but pathology-positive lesion was labeled as false negative (FN). Figure 2 shows an example of our radiology-pathology correlation analysis with mpMRI and WMHP and the procedure for labeling lesions as TP, FP, and FN when different criteria are applied. Figure 2a shows two MRI lesions, with PI-RADS 4 and 3, and two pathology lesions with ISUP grades of 3 (GS 4+3=7) and 1 (GS 3+3=6). Comparing lesions on MRI and WMHP shows that lesion #1

appeared on both MRI and WMHP. In contrast, lesion #2 was only positive on MRI, and lesion #3 was only positive on WMHP. We show examples of the different definitions of TP/FP/FN when MRI positives are defined as PI-RADS ≥ 3 and pathology positives as ISUP grade ≥ 1 (Figure 2b) and when MRI positives are defined as PI-RADS ≥ 4 and pathology positives as ISUP grade ≥ 2 (Figure 2c). It is notable that pathology-positive lesions with ISUP>=2 were considered as csPCa. The final number of PCa lesions represents the sum of all lesions identified by WMHP (i.e., TP+FN).

The location of each lesion (TP, FP, and FN) was recorded on sector map, which is a segmentation model of prostate anatomic zones and levels, used in Prostate Imaging Reporting and Data System version 2.1 (PI-RADSv2.1). It employs forty-one sectors/regions: thirty-eight for the prostate, two for the seminal vesicles, and one for the external urethral sphincter, to enable radiologists, urologists, pathologists, and others to localize findings described in MRI reports (Fig. 3).

Statistical Analysis

All data were statistically analyzed using SPSS v26.0 (IBM Corp, Armonk, NY, USA). The diagnostic performance of mpMRI between matched W and AA men was assessed by calculating detection rates, DR=TP/(TP+FN), and positive predictive values, PPV=TP/(TP+FP). The location of each lesion (TP, FP, and FN) was recorded on the sector map described by PI-RADS v2.1, and the number of each TP, FN and FP lesions was normalized by the number of sectors in which the lesion was distributed. Collecting the per-lesion-based location information yielded the weighted sum of TP, FP, and FN lesions in each sector, which was used to obtain the per-lesion diagnostic performance of mpMRI (DR and PPV) in both AA and W men.

Baseline patient demographics between AA and matched W men were compared using the Mann-Whitney U test for continuous variables. The number of PCa lesions relative cancer prevalence(rCP), DR, and PPV values were calculated for each sector, and the diagnostic performances for each prostate zone (transition zone; TZ or peripheral zone; PZ) and anterior/posterior prostate were determined by aggregating the sectors corresponding to these regions. The weighted Pearson's chi-square test was performed to examine the statistical differences between AA and matched W men for the categorical variables, including DR and PPV, in which the weighted sum of each variable was adjusted by the number of observations. A P-value less than 0.05 was considered statistically significant.

RESULTS

Tables 1 and 3 show the patient and lesion characteristics after matching the propensity score with age, PSA, and prostate volume between AA and W men. Among the 264 PCa lesions on WMHP, 98 and 166 lesions were identified in AA and W sub-cohorts, respectively. The average number of pathology-based lesions per patient for AA men was 2.28, which is higher than that (1.93) for matched W men (P=0.46). Among the 145 MRI-positive lesions, the average number of MRI-based lesions per patient for AA men was 1.05, which was slightly lower than 1.16 for matched W men (P=0.68).

Diagnostic performances of csPCa (ISUP grade ≥ 2) lesions between AA and matched W sub-cohorts are shown in Table 4. Higher cancer prevalence was observed in PZ than TZ, and the trend was higher for AA men (18.7%; TZ vs. 77.7%; PZ) than for the matched W men (33.6%; TZ vs. 60.5%; PZ). There were no significant differences in DRs in AA and matched W sub-cohorts (Table 4), except for csPCa lesions in the posterior part of the prostate (75.3%; AA vs. 64.4%; W,

P=0.03). Similar patterns were observed in PPVs; csPCa lesions in PZ and the posterior part of the prostate had significantly higher PPVs for AA men than those for the matched W men.

The sector-based spatial characteristics of csPCa lesions are shown for AA men (Figure 3) and matched W men (Figure 4). The rCP, DR, and PPV values are shown in each prostate sector, with different colors highlighting the sectors belonging to different percentiles across 41 sectors of the prostate. The sectors belonging to the 75^{th} percentile and higher rCP, and the 25^{th} percentile and lower DR and PPV, are shown in red. The figures show that posterior tumors at the apex level of the prostate had relatively lower DRs for the AA men and the matched W men.

Quantitative DCE-MRI (K^{trans} and v_e) and ADC parameters in AA and matched W sub-cohorts are summarized in Table 5. Significant differences between the two cohorts were observed in the K^{trans} and v_e of tumors with various ISUP grades. Additionally, the tumors of AA men had significantly higher K^{trans} than the matched W sub-cohort when the PI-RADS score was ≥ 3 or ≥ 4. However, the ADC values were not significantly different between the two races (all p-values reported in Table 5). Figure 5 shows boxplots of K^{trans}, v_e, and ADC of AA and matched W sub-cohorts for csPCa lesions, (a) ISUP grades ≥ 2, and (b) index ISUP grades ≥ 2.

DISCUSSION

AA men present with higher PSA values (9,13), more advanced PCa and age-adjusted PCa mortality rate than W men (29). A recent study including 600 patients showed that PCa detection using PI-RADS was not significantly different between AA and W sub-cohorts (20). However, another previous study (n=194) reported that AA men were at a significantly higher risk of having csPCa when mpMRI was negative (PI-RADS 1 or 2) (30). These results indicate that the current PI-RADS-based interpretation may not be sensitive enough to account for underlying ethnic/race-

specific biological differences in PCa. In this study, we found that K^{trans} and v_e were significantly higher in AA men than in W men with PCa, while age, PSA, and prostate volume were not significantly different. Thus, the differences in microvascular perfusion between AA and W sub-cohorts may further benefit the understanding and characteristics of PCa.

The racial difference in K^{trans} was significant in the PCa of ISUP 2 or 3, but not in ISUP 1. The highest difference in K^{trans} between AA and matched W sub-cohorts was observed for ISUP 3 PCa. Furthermore, when categorizing lesions based on PI-RADS scores, K^{trans} was significantly different between AA and W men in the lesions with PI-RADS ≥ 3, but not in those with PI-RADS 3, confirming that PCa malignancy in lesions with PI-RADS 3 classification is uncertain.

The difference in K^{trans} and v_e between AA and W men could reflect imaging phenotypes associated with differences in tumor microvascular environment among men from different racial backgrounds, as suggested by several studies investigating genetic/epigenetic factors and the influence of the tumor microenvironment (7,8,31). If present, any race-based parameters that reflect differences in tumor biology could be used to improve diagnosis in AA men, especially when interpreting mpMRI. A more refined, lesion-specific approach may also be considered to further improve csPCa detection, as studies have reported differences between TZ and PZ in the perfusion characteristics (32). This may imply the importance of including DCE-MRI in mpMRI, particularly for AA men.

PI-RADS guidelines include different review criteria based on prostate zonal anatomy, and studies have reported different diagnostic performances of mpMRI between TZ and PZ (33,34). Investigating race-based information concerning prostate zonal anatomy may help clinical decisions by accounting for these variations. We believe this may create future research that can

improve diagnostic performances of mpMRI by incorporating prior knowledge into learning-based methods (35).

Although this research aimed to investigate differences in mpMRI performances between AA and W men, the outcomes encourage the expansion of the study to include other races as well. However, performing such studies heavily depends on the demography of the population where the institute is located. Moreover, radiology-pathology correlation entails using WMHP slides, which is not a standard routine in clinical practices and only is performed in a few centers around the world further limiting data collection via collaboration and multi-center studies.

Limitations

Firstly, the cohort of AA men after matching commonly known clinical risk factors was relatively small. The initial study cohort comprised 942 patients who underwent mpMRI before prostatectomy with <5% being AA men, while the rest were mostly W men. Future studies may include performing a multi-institutional evaluation to bolster sample sizes and improve generalizability. Secondly, this was a retrospective study with inherent biases. In particular, the WMHP analysis required a surgical population and consequently introduced a selection bias. However, histopathological findings via MRI/transrectal ultrasound fusion-guided biopsy commonly have high uncertainty due to biopsy sampling error, interpretation variability, and lesions with borderline grades. Studies have reported that more than 30% of the cases were upgraded, and more than 25% were downgraded following protastectomy, compared to WMHP (36,37). Moreover, without WMHP, including false-negative lesions in assessing the diagnostic performances and spatial characteristics of prostate cancer lesions are not possible. Therefore, despite the potential for selection bias, the matching of postoperative WMHP to MRI enabled an

accurate pathological assessment and image analysis (38). Lastly, the variability in qDCE measurement across different institutions and vendors remains a concern for the accurate and reproducible application of qDCE (39). Kim et al. recently demonstrated that the specificity of K^{trans} to detect csPCa was improved from 86% to 93% using a phantom-based error correction method (40). Regardless, significant differences in K^{trans} have been observed, and future studies may increase the reproducibility of qDCE further.

Conclusion

This study showed differences in the diagnostic performance of mpMRI and spatial characteristics of prostate cancer between AA and W men after matching known clinical risk factors. This racial difference was also observed in the K^{trans} tumor characteristic of microvascular perfusion in both pathology- and MRI-based prostate cancer lesions, while differences were not seen in age, PSA, and prostate volume. This finding may reflect differences in tumor biology and the potential use of race-based imaging may further improve diagnosis in AA men, especially when interpreting mpMRI.

ACKNOWLEDGEMENT

This research was funded in part by the National Institutes of Health under grants R01-CA248506 and R01-CA272702 and by the Integrated Diagnostics Program of the Departments of Radiological Sciences and Pathology in the UCLA David Geffen School of Medicine.

REFERENCES

[1] Attard, G. et al. Prostate cancer. *Lancet.* 2016;387:70-82. doi: 10.1016/s0140-6736(14)61947-4.

[2] Riviere, P. et al. Survival of African American and non-Hispanic white men with prostate cancer in an equal-access health care system. *Cancer.* 2020;126:1683-1690. doi: 10.1002/cncr.32666.

[3] Siegel, D.A., O'Neil, M.E., Richards, T.B., Dowling, N.F., Weir, H.K. Prostate Cancer Incidence and Survival, by Stage and Race/Ethnicity - United States, 2001-2017. *MMWR Morb Mortal Wkly Rep.* 2020;69:1473-1480. doi: 10.15585/mmwr.mm6941a1.

[4] Borno, H. et al. All Men Are Created Equal: Addressing Disparities in Prostate Cancer Care. *Am Soc Clin Oncol Educ Book.* 2019;39:302-308. doi: 10.1200/edbk_238879.

[5] Friedlander, D.F. et al. Racial Disparity in Delivering Definitive Therapy for Intermediate/High-risk Localized Prostate Cancer: The Impact of Facility Features and Socioeconomic Characteristics. *Eur Urol.* 2018;73:445-451. doi: 10.1016/j.eururo.2017.07.023.

[6] Ziehr, D.R. et al. Income inequality and treatment of African American men with high-risk prostate cancer. *Urol Oncol.* 2015;33:18.e17-18.e13. doi: 10.1016/j.urolonc.2014.09.005.

[7] Bhardwaj, A. et al. Racial disparities in prostate cancer: a molecular perspective. *Front Biosci (Landmark Ed)*. 2017;22:772-782. doi: 10.2741/4515.

[8] Wallace, T.A. et al. Tumor immunobiological differences in prostate cancer between African-American and European-American men. *Cancer Res*. 2008;68:927-936. doi: 10.1158/0008-5472.Can-07-2608.

[9] Smith, Z.L., Eggener, S.E., Murphy, A.B. African-American Prostate Cancer Disparities. *Curr Urol Rep*. 2017;18:81. doi: 10.1007/s11934-017-0724-5.

[10] Craciunescu, O.I. et al. DCE-MRI parameters have potential to predict response of locally advanced breast cancer patients to neoadjuvant chemotherapy and hyperthermia: a pilot study. *Int J Hyperthermia*. 2009;25:405-415. doi: 10.1080/02656730903022700.

[11] Kim, H. et al. Early therapy evaluation of combined cetuximab and irinotecan in orthotopic pancreatic tumor xenografts by dynamic contrast-enhanced magnetic resonance imaging. *Mol Imaging*. 2011;10:153-167.

[12] Mano, R., Eastham, J., Yossepowitch, O. The very-high-risk prostate cancer: a contemporary update. *Prostate Cancer Prostatic Dis.* 2016;19:340-348. doi: 10.1038/pcan.2016.40.

[13] Yuan, Q. et al. Quantitative diffusion-weighted imaging and dynamic contrast-enhanced characterization of the index lesion with multiparametric MRI in prostate cancer patients. *Journal of magnetic resonance imaging : JMRI*. 2017;45:908-916. doi: 10.1002/jmri.25391.

[14] Futterer, J.J. et al. Staging prostate cancer with dynamic contrast-enhanced endorectal MR imaging prior to radical prostatectomy: experienced versus less experienced readers. *Radiology*. 2005;237:541-549. doi: 10.1148/radiol.2372041724.

[15] Abdalla, I., Ray, P., Ray, V., Vaida, F., Vijayakumar, S. Comparison of serum prostate-specific antigen levels and PSA density in African-American, White, and Hispanic men without prostate cancer. *Urology*. 1998;51:300-305. doi: Doi 10.1016/S0090-4295(97)00617-1.

[16] Klein, E. A., & Patel, A. R. Risk factors for prostate cancer. *Nature Clinical Practice Urology*. 2009;6:87–95. https://doi.org/10.1038/ncpuro1290.

[17] Ibraheem, A., Olopade, O.I., Huo, D. Propensity score analysis of the prognostic value of genomic assays for breast cancer in diverse populations using the National Cancer Data Base. *Cancer*. 2020;126(17):4013-4022.

[18] Azin, A., Guidolin, K., Chadi, S.A., Quereshy, F.A. Racial disparities in colon cancer survival: A propensity score matched analysis in the United States. *Surgery.* 2022;171(4):873-881.

[19] Deebajah, M. et al. A propensity score matched analysis of the effects of African American race on the characteristics of regions of interests detected by magnetic resonance imaging of the prostate. *Urol Oncol.* 2019;37(8):531.e1-531.e5.

[20] Henning, G.M. et al. Diagnostic Performance of Prostate Multiparametric Magnetic Resonance Imaging in African-American Men. *Urology*. 2019;134:181-185.

[21] Egevad, L., Delahunt, B., Srigley, J.R., Samaratunga, H. International Society of Urological Pathology (ISUP) grading of prostate cancer - An ISUP consensus on contemporary grading. APMIS. 2016;124:433-5. doi: 10.1111/apm.12533.

[22] American College of Radiology. PI-RADSTM prostate imaging reporting and data system. Amsterdam, Netherlands: Elsevier;2019.Available from: https://www.acr.org/-/media/ACR/Files/RADS/Pi-RADS/PIRADS-V2-1.pdf.

[23] Vajuvalli, N.N. et al. The Tofts model in frequency domain: fast and robust determination of pharmacokinetic maps for dynamic contrast enhancement MRI. *Phys. Med. Biol*. 2016;61: 8462. DOI 10.1088/0031-9155/61/24/8462.

[24] Parker, G.J. et al. Experimentally-derived functional form for a population-averaged high-temporal-resolution arterial input function for dynamic contrast-enhanced MRI. *Magn Reson Med*. 2006;56:993-1000. doi: 10.1002/mrm.21066.

[25] Tofts, P.S. et al. Estimating kinetic parameters from dynamic contrast-enhanced T(1)-weighted MRI of a diffusable tracer: standardized quantities and symbols. *J Magn Reson Imaging.* 1999;10:223-232. doi: 10.1002/(sici)1522-2586(199909)10:3<223::aid-jmri2>3.0.co;2-s.

[26] Chao, S.L., Metens, T., Lemort. M. TumourMetrics: a comprehensive clinical solution for the standardization of DCE-MRI analysis in research and routine use. *Quant Imaging Med Surg*. 2017; 7:496–510. doi: 10.21037/qims.2017.09.02.

[27] van Leenders, G. et al. The 2019 International Society of Urological Pathology (ISUP) Consensus Conference on Grading of Prostatic Carcinoma. *Am J Surg Pathol*. 2020;44:e87-e99. doi: 10.1097/PAS.0000000000001497.

[28] Jackson, A., O'Connor, J.P.B., Parker, G.J.M., Jayson, G.C. Imaging Tumor Vascular Heterogeneity and Angiogenesis using Dynamic Contrast-Enhanced Magnetic Resonance Imaging. *Clin Cancer Res.* 2007;13:3449–3459.

[29] QuickStats: Age-Adjusted Death Rates* from Prostate Cancer,(dagger) by Race/ Ethnicity - National Vital Statistics System, United States, 1999-2017. *MMWR Morb Mortal Wkly Rep*. 2019;68:531. doi: 10.15585/mmwr.mm6823a4.

[30] Kuhlmann, P.K. et al. Patient- and tumor-level risk factors for MRI-invisible prostate cancer. *Prostate Cancer Prostatic Dis*. 2021;24:794-801. doi: 10.1038/s41391-021-00330-7.

[31] Hötker, A.M. et al. Assessment of Prostate Cancer Aggressiveness by Use of the Combination of Quantitative DWI and Dynamic Contrast-Enhanced MRI. *AJR Am J Roentgenol*. 2016;206:756-763. doi: 10.2214/ajr.15.14912.

[32] Sung. K. Modified MR dispersion imaging in prostate dynamic contrast-enhanced MRI. *J Magn Reson Imaging*. 2019;50:1307-1317. doi: 10.1002/jmri.26685.

[33] Gaur, S. et al. Can computer-aided diagnosis assist in the identification of prostate cancer on prostate MRI? a multi-center, multi-reader investigation. *Oncotarget.* 2018; 9:33804-33817. https://doi.org/10.18632/oncotarget.26100.

[34] Wibulpolprasert, P. et al. Influence of the Location and Zone of Tumor in Prostate Cancer Detection and Localization on 3-T Multiparametric MRI Based on PI-RADS Version 2. *AJR Am J Roentgenol.* 2020;214:1101-1111. 10.2214/AJR.19.21608.

[35] Gulcehre, C. and Bengio, Y. Knowledge Matters: Importance of Prior Information for Optimization. *J Machine Learning Research*. 2016;17:1-32. https://arxiv.org/abs/1301.4083.

[36] Epstein, J.I., Feng, Z., Trock, B.J., Pierorazio, P.M. Upgrading and downgrading of prostate cancer from biopsy to radical prostatectomy: incidence and predictive factors using the modified Gleason grading system and factoring in tertiary grades. *Eur Urol.* 2012;61:1019-1024.

[37] D'Elia, C., Cerruto, M.A., Cioffi, A., Novella, G., Cavalleri, S., Artibani, W. Upgrading and upstaging in prostate cancer: From prostate biopsy to radical prostatectomy. *Mol Clin Oncol.* 2014;2:1145-1149. doi: 10.3892/mco.2014.370.

[38] Le, J.D. et al. Multifocality and prostate cancer detection by multiparametric magnetic resonance imaging: correlation with whole-mount histopathology. *Eur Urol.* 2015;67:569-576.

[39] Kim, H. Variability in Quantitative DCE-MRI: Sources and Solutions. *J Nat Sci*. 2018;4.

[40] Kim, H. et al. Portable perfusion phantom for quantitative DCE-MRI of the abdomen. *Med Phys*. 2017;44:5198-5209. doi: 10.1002/mp.12466.

Tables

Table 1. Patient characteristics between AA and W men after the propensity score matching.

	African American (N=43)	White men (matched; N=86)	P-value
Age years median (IQR)	61.9 (56.5-66.0)	62.6 (56.7-67.9)	0.77
PSA ng/ml median (IQR)	6.8 (5.8-8.3)	6.5 (4.3-10.2)	0.79
PSAD ng/ml/cc median (IQR)	0.16 (0.12-0.21)	0.14 (0.09-0.27)	0.38
PV cc median (IQR)	41 (34.3-54)	38.6 (30-50.2)	0.30

All *p*-values were derived from Mann-Whitney U tests.

PSA = prostate-specific antigen; PSAD = prostate-specific antigen density; PV = prostate volume.

Table 2: The detailed mpMRI sequence parameters.

MRI Sequence	Spatial Resolution (mm × mm)	Slice Thickness (mm)	Matrix Size	Field-of-View (mm^2)	TR/TE (ms)	b-values (s/mm^2)
T2W	0.65 × 0.65	3.0	380 × 380	208 × 208	4000 / 109	-
DWI	1.6 × 1.6	3.6	160 × 94	260 × 216	3600 / 80	0, 100, 400, 800, and (calculated) 1,400
DCE	1.6 × 1.6	3.6	160 × 160	260 × 260	4.2 / 1.5	-

MRI = magnetic resonance imaging; T2W = T2-weighted; DWI = diffusion-weighted imaging; DCE = dynamic contrast-enhanced.

Table 3: Lesion characteristics between AA and W men after the propensity score matching.

		ALL	African American men	White men (matched)	P-value
Number of patients		129	43	86	-
Pathology-based Lesion	**Number of lesions (lesions/patient)**	264 (2.05)	98 (2.28)	166 (1.93)	0.46
	Solitary PCa lesions (lesions/patient)	46	14 (0.33)	32 (0.37)	0.72
	Multifocal PCa lesions (lesions/patient)	218	84 (1.95)	134 (1.56)	0.33
	ISUP grade 1 (lesions/patient)	94	37 (0.86)	57 (0.66)	0.35
	ISUP grade 2 (lesions/patient)	112	40 (0.93)	72 (0.84)	0.70
	ISUP grade 3 (lesions/patient)	36	11 (0.26)	25 (0.29)	0.75
	ISUP grade ≥ 4 (lesions/patient)	22	10 (0.23)	12 (0.14)	0.27
MRI-based Lesion	**Number of lesions (lesions/patient)**	145 (1.12)	45 (1.05)	100 (1.16)	0.68
	PI-RADS 3 (lesions/patient)	29	8 (0.19)	21 (0.24)	0.55
	PI-RADS ≥ 4 (lesions/patient)	116	37 (0.86)	79 (0.92)	0.81

All *p*-values were derived from Pearson's chi-square tests.

Table 4: Diagnostic performance of mpMRI for detecting clinically significant PCa lesions in AA and matched W men.

Diagnostic performance of mpMRI			African American men	White men (matched)	P-value
ISUP grade ≥ 2 & PI-RADS ≥ 3	No. Lesions (TP/FN/FP)		60 (39/10/11)	125 (64/34/27)	-
	Relative Cancer Prevalence (%)	Transition Zone	18.7	33.9	-
		Peripheral Zone	77.7	60.5	
	Detection Rate (%)	All Pathology-based Lesions	81.6	75.0	0.11
		Transition Zone	81.3	79.1	0.79
		Peripheral Zone	80.8	72.5	0.10
		Anterior	77.8	79.9	0.80
		Posterior	82.4	72.0	0.03*
	PPV (%)	All MRI-based Lesions	83.2	71.9	<0.001**
		Transition Zone	67.8	79.5	0.16
		Peripheral Zone	87.8	68.1	<0.001**
		Anterior	64.0	75.6	0.17
		Posterior	89.3	69.6	0.007**

All *p*-values were derived from weighted Pearson's chi-square tests.

* $P < 0.05$ and ** $P < 0.01$.

Table 5: Quantitative mpMRI characteristics between African American and White men.

		K^{trans} (min^{-1} × 1,000)			v_e			ADC (10^{-6} mm^2/s)		
		African American men	**White men (matched)**	**P-value**	**African American men**	**White men (matched)**	**P-value**	**African American men**	**White men (matched)**	**P-value**
Pathology-based Lesions	**ISUP grade=1**	198.8 ± 94.7	177.3 ± 162.5	0.61	0.373 ± 0.158	0.312 ± 0.162	0.42	938.5 ± 215.2	910.3 ± 138.9	0.74
	ISUP grade=2	230.5 ± 69.8	193.7 ± 75.9	**0.02***	0.368 ± 0.147	0.327 ± 0.123	0.25	884.5 ± 214.1	894.9 ± 168.7	0.84
	ISUP grade=3	274.7 ± 220.8	178.5 ± 77.0	**0.06***	0.349 ± 0.204	0.288 ± 0.084	0.31	1029.5 ± 322.9	890.4 ± 155.3	0.16
	ISUP grade≥1	227.0 ± 108.7	190.7 ± 112.0	**0.03***	0.374 ± 0.158	0.316 ± 0.119	0.03*	918.7 ± 222.1	875.2 ± 163.0	0.23
	ISUP grade≥2	237.4 ± 112.5	196.0 ± 84.7	**0.01****	0.374 ± 0.161	0.316 ± 0.113	0.04*	912.3 ± 227.4	870.6 ± 166.2	0.31
	ISUP grade≥2 (Index)	250.7 ± 122.1	196.7 ± 84.7	**0.008****	0.391 ± 0.139	0.320 ± 0.109	0.02*	881.7 ± 202.4	857.9 ± 155.9	0.59
MRI-based Lesions	**PI-RADS=3**	193.6 ± 91.0	201.5 ± 139.5	0.90	0.188 ± 0.084	0.343 ± 0.179	0.25	792.5 ± 37.5	995.5 ± 163.9	0.10
	PI-RADS≥3	237.9 ± 122.1	198.4 ± 97.6	**0.046***	0.347 ± 0.133	0.314 ± 0.115	0.24	884.2 ± 184.8	879.7 ± 164.5	0.91
	PI-RADS≥4	245.5 ± 126.2	197.6 ± 84.9	**0.02***	0.362 ± 0.127	0.306 ± 0.091	0.03*	892.9 ± 191.2	848.5 ± 151.1	0.27

All *p*-values were derived from Mann-Whitney U tests.

* $P < 0.05$ and ** $P < 0.01$.

Figure Legends

Figure 1: The inclusion workflow of the study population.

Figure 2: Radiology-pathology correlation using (a) mpMRI and WMHP, and illustration of true positive (TP), false positive (FP) and false negative (FN) lesions with different MRI/histopathological finding groups: (b) ISUP grade ≥ 1 with PI-RADS ≥ 3 (detection rate = 50% and PPV = 50%) or (c) ISUP grade ≥ 2 with PI-RADS ≥ 4 (detection rate = 100% and PPV = 100%).

Figure 3: Spatial characteristics of csPCa (ISUP grade ≥ 2) lesions for AA men, including relative cancer prevalence (rCP), detection rate (DR) and positive predictive value (PPV) heatmaps at the basal, mid, and apex levels, corresponding to prostate sector map. The red color indicates the 75th percentile or higher of rCP and the 25th percentile or lower of DR and PPV values on the sector map.

Figure 4: Spatial characteristics of csPCa (ISUP grade ≥ 2) lesions for matched W men, including relative cancer prevalence (rCP), detection rate (DR) and positive predictive value (PPV) heatmaps at the basal, mid, and apex levels, corresponding to prostate sector map. The red color indicates the 75th percentile or higher of rCP and the 25th percentile of lower of DR and PPV on the sector map.

Figure 5: Quantitative DCE parameters and ADC for csPCa lesions in African American and matched White men.

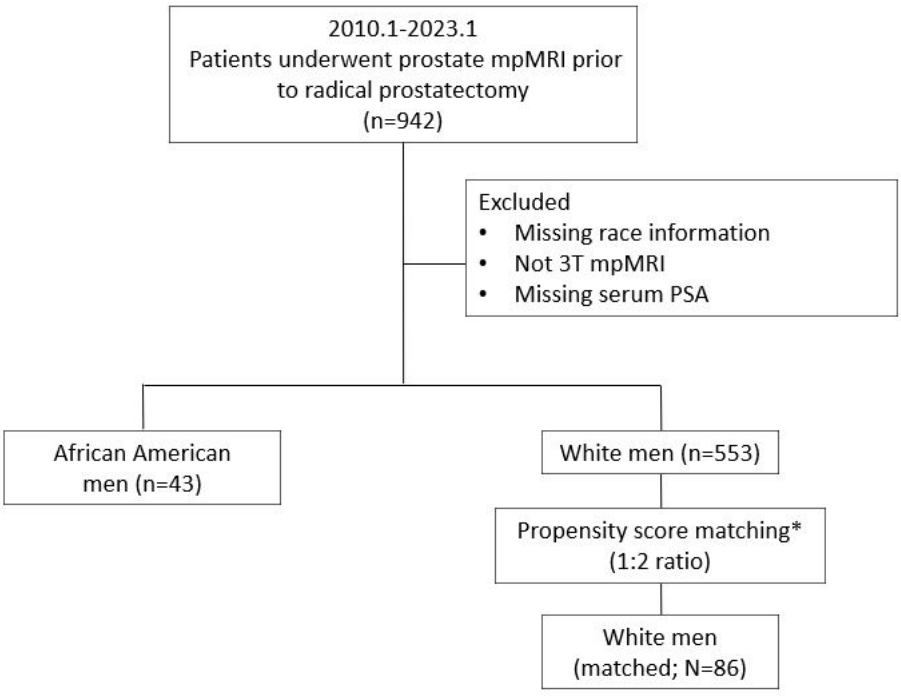

Figure 1: The inclusion workflow of the study population.

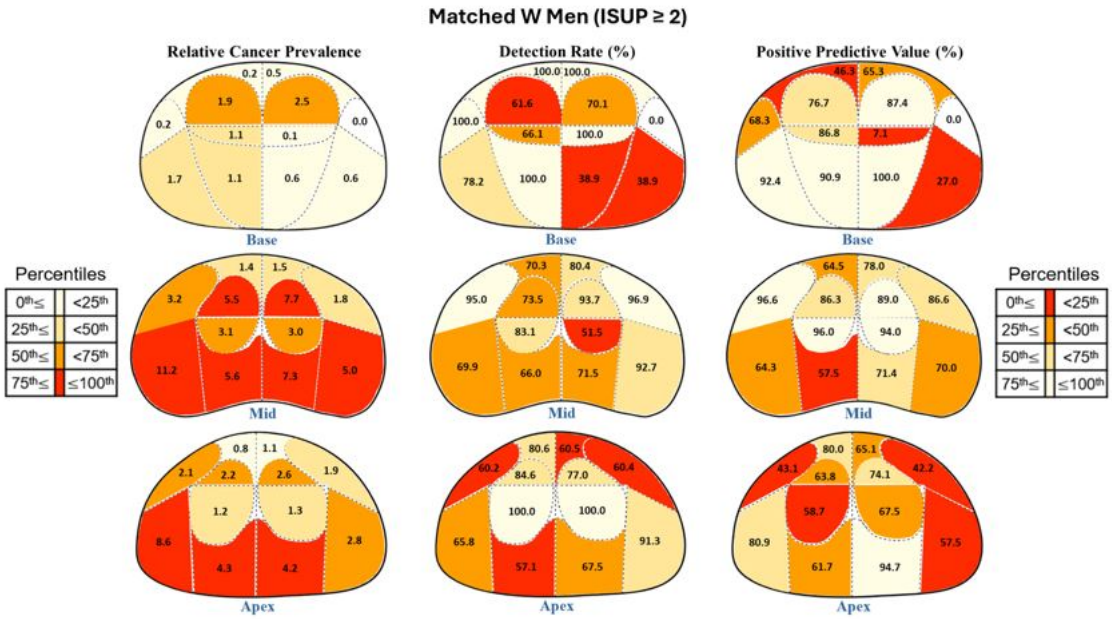

Figure 2: Radiology-pathology correlation using (a) mpMRI and WMHP, and illustration of true positive (TP), false positive (FP) and false negative (FN) lesions with different MRI/histopathological finding groups: (b) ISUP grade ≥ 1 with PI-RADS ≥ 3 (detection rate = 50% and PPV = 50%) or (c) ISUP grade ≥ 2 with PI-RADS ≥ 4 (detection rate = 100% and PPV = 100%).

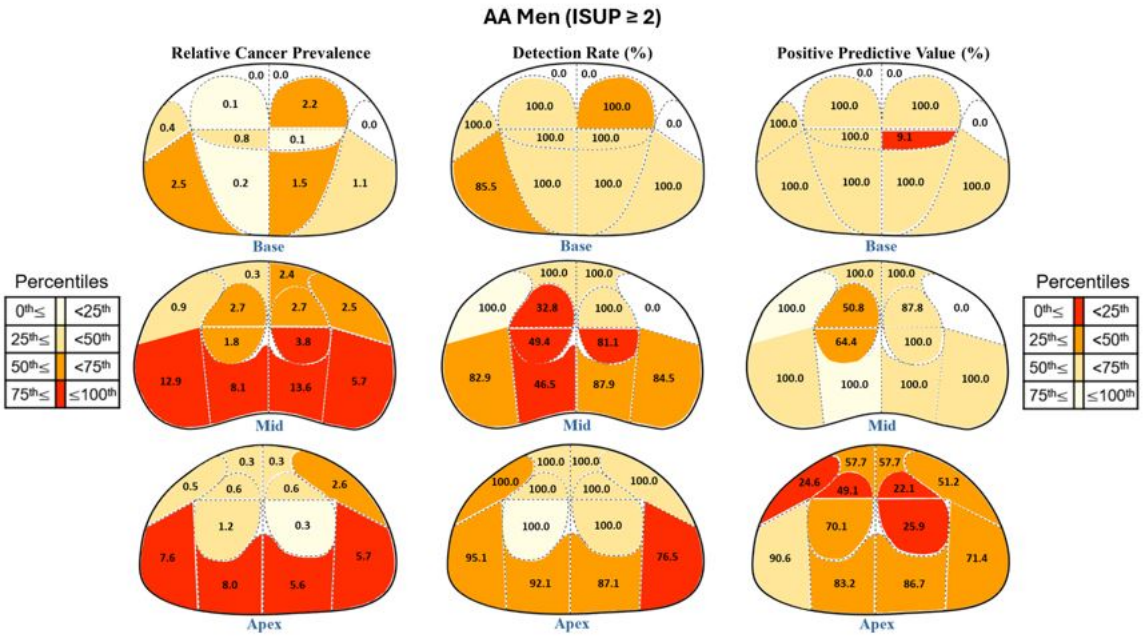

Figure 3: Spatial characteristics of csPCa (ISUP grade ≥ 2) lesions for AA men, including relative cancer prevalence (rCP), detection rate (DR) and positive predictive value (PPV) heatmaps at the basal, mid, and apex levels, corresponding to prostate sector map. The red color indicates the 75th percentile or higher of rCP and the 25th percentile or lower of DR and PPV values on the sector map.

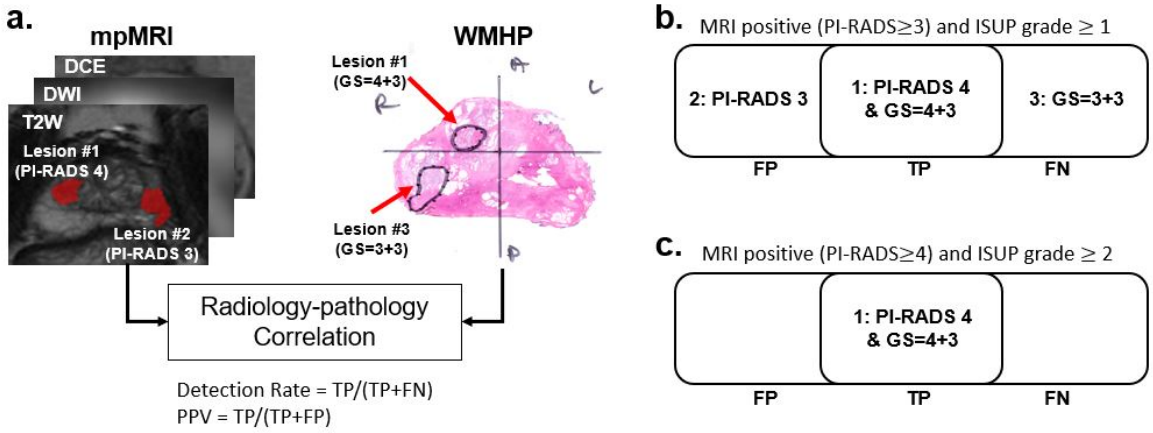

Figure 4: Spatial characteristics of csPCa (ISUP grade ≥ 2) lesions for matched W men, including relative cancer prevalence (rCP), detection rate (DR) and positive predictive value (PPV) heatmaps at the basal, mid, and apex levels, corresponding to prostate sector map. The red color indicates the 75th percentile or higher of rCP and the 25th percentile of lower of DR and PPV on the sector map.

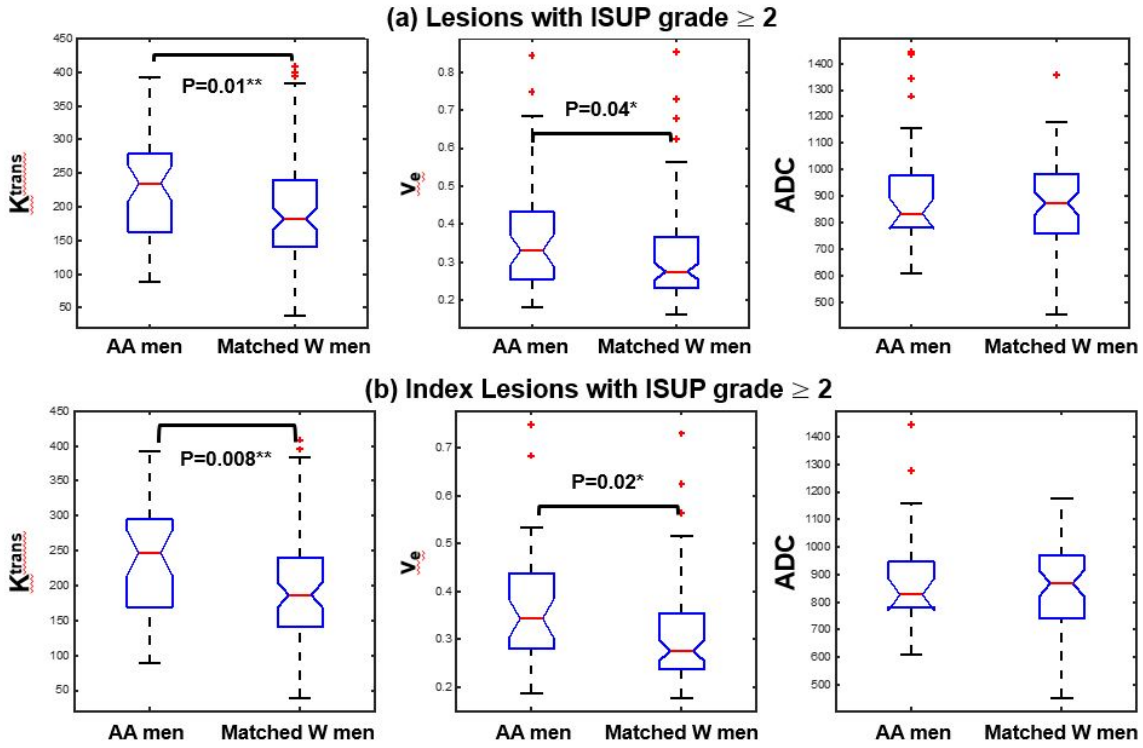

Figure 5: Quantitative DCE parameters and ADC for csPCa lesions in African American and matched White men.